



HAL
open science

Experimental Study of a Lyotropic Lamellar Phase Swollen with Polymer Solutions

M.-F. Ficheux, A.-M. Bellocq, F. Nallet

► **To cite this version:**

M.-F. Ficheux, A.-M. Bellocq, F. Nallet. Experimental Study of a Lyotropic Lamellar Phase Swollen with Polymer Solutions. *Journal de Physique II*, 1995, 5 (6), pp.823-834. 10.1051/jp2:1995167 . jpa-00248202

HAL Id: jpa-00248202

<https://hal.science/jpa-00248202>

Submitted on 4 Feb 2008

HAL is a multi-disciplinary open access archive for the deposit and dissemination of scientific research documents, whether they are published or not. The documents may come from teaching and research institutions in France or abroad, or from public or private research centers.

L'archive ouverte pluridisciplinaire **HAL**, est destinée au dépôt et à la diffusion de documents scientifiques de niveau recherche, publiés ou non, émanant des établissements d'enseignement et de recherche français ou étrangers, des laboratoires publics ou privés.

Classification

Physics Abstracts

82.70-y — 64.70Md — 61.25Hq

Experimental Study of a Lyotropic Lamellar Phase Swollen with Polymer Solutions

M.-F. Ficheux, A.-M. Bellocq and F. Nallet

Centre de recherche Paul-Pascal, CNRS, avenue du Docteur-Schweitzer, 33600 Pessac, France

(Received 27 January 1995, accepted 27 February 1995)

Abstract. — We report on the effect of a hydrosoluble neutral polymer on the stability of a lamellar phase made of charged surfactant bilayers. In the system investigated, the smectic structure exists for a wide range of dilutions, with smectic periods continuously varying between 30 and 300 Å. Our results show that the lamellar structure still exists when pure water is replaced with aqueous solutions of polyethyleneglycol (PEG: radius of gyration $R_g = 29$ Å, molecular weight $M_w = 22600$ g/mol). Large amounts of PEG can be solubilized in the mesophase: up to 50% of the water can be replaced by the polymer. However, the added polymer causes a reduction in the swelling of the phase and most remarkably produces at intermediate polymer and bilayer concentrations a phase separation between two lamellar phases of different periods. We have studied the system with static (X-ray or neutron) and dynamic (light) scattering techniques. The polymer gets partially associated to the surfactant bilayer, as revealed by the small decrease of the smectic spacing as a function of PEG concentration at constant surfactant-cosurfactant volume fractions. Besides, the interactions between bilayers are less repulsive in the presence of PEG than the weakly-screened electrostatic repulsion expected with our ionic surfactant. Interactions may even become attractive, which leads to a phase separation between two lamellar phases. The decrease in the layer compression modulus \bar{B} is studied through its consequences on Bragg peak linewidth, small angle scattering and baroclinic mode relaxation frequency. The eventual presence of critical points on the border of the closed-loop smectic-smectic miscibility gap is investigated

1. Introduction

An increasing interest is directed today towards polymer/surfactant systems for technical reasons as well as for the intriguing features displayed by such systems. It has been recognized that polymers may significantly alter the properties of self-assembled surfactant structures in solution and their interactions [1] but our fundamental understanding of these changes is still rather restricted. Most of the studies have concentrated on systems composed of water soluble uncharged polymers and ionic surfactants. Polyethylene oxide (PEO) is one of such water soluble neutral polymers that has been extensively studied in anionic surfactant solutions. In the case of PEO-sodium dodecylsulphate (SDS), Cabane and Duplessix [2] have shown that

in bulk solution micelles adsorb onto the polymer chain forming a necklace-type structure. In addition, it has been found that at high surfactant concentration (75% SDS) a periodic layered structure for the polymer is produced by dissolution of PEO in the SDS lamellar phase [3]. Recently, the role of added polymer in dilute lamellar phases has also been investigated theoretically [4–6] and experimentally [7, 8]. The effects of the polymer on the bilayer bending elasticity have been predicted and the phase diagrams calculated for various conditions of polymer adsorption, flexibility of the bilayers and bilayer interactions [6].

Ionic surfactant-alcohol-water mixtures [9–11] seem to us appropriate systems in which to investigate the interaction between surfactant bilayers and polymer. Indeed, in the lamellar phase of these systems, by addition of solvent it is possible to vary the repeat distance d continuously from molecular sizes (20 Å) to extremely large distances (100–1000 Å). In the following we describe the effect of polyethyleneglycol (PEG) on the stability of the lamellar phase of the water-SDS-octanol system using scattering techniques (light, neutrons and X-rays).

2. Experimental Part

2.1. SAMPLE PREPARATION. — Sodium dodecylsulphate (SDS) purchased from Touzart and Matignon was recrystallized from absolute ethanol. Octanol was used as received from Aldrich. The polymer was obtained from Fluka and used without further purification. We measured its molecular weight by gel permeation chromatography: $M_w = 22600$ g/mol; polydispersity index $M_w/M_n = 1.1$. PEG/water mixtures form clear solutions at 25 °C in the whole range of compositions investigated, 0–50 wt%. The radius of gyration of isolated PEG macromolecules in water R_g and the overlap concentration c^* , deduced from neutron and light scattering measurements are 29 Å and 35 g/l, respectively [12]. The preparation of spatially homogeneous samples at thermodynamic equilibrium is crucial in the study of polymer-containing mesophases. In order to achieve this result the samples with the largest membrane concentrations were prepared by mixing surfactant, alcohol and stock solutions of the polymer in water. The sample tubes were then centrifuged several times, equilibrated at 25 °C for several days. Most of our more dilute samples were then prepared by diluting the initial concentrated samples with aqueous solutions at several fixed polymer concentrations, i.e. along “dilution lines”. At that stage, a first indication of the nature of the phases is obtained by visual observation of the tubes between crossed polarizers, which shows whether the sample is homogeneously birefringent, or if a phase separation occurs between isotropic and birefringent phases. For samples close to phase separation, a second observation using optical microscopy is required in order to confirm the expected lamellar texture, without any trace of residual isotropic droplets. The criterion finally used to judge whether a birefringent sample is at thermodynamic equilibrium was the reproducibility of its X-ray spectrum

2.2. INSTRUMENTS

2.2.1. X-ray. — Our X-ray set-up is built with a 18 kW copper rotating anode source (Rigaku), operated usually at 50 kV and 240 mA. A graphite monochromator set for the (002) reflection selects the copper K_α line with wavelength $\lambda = 1.54$ Å (together with lower intensity harmonics at λ/n from the Bremsstrahlung background). The incident beam is collimated by a set of rectangular slits that define an irradiated area on the sample 0.8×1 mm². We use a 2D-image plate detector (Mar Research); the detection area, of circular shape with diameter 18 cm, is an assembly of square pixels with dimensions 150×150 μm² providing a 16-bit dynamic range. The direct beam is blocked in front of the detector by a beam stop with diameter 1.2 cm. With

a sample-to-detector distance of 1.18 m, the nominal wave vector range extends from 0.02 \AA^{-1} to 0.30 \AA^{-1} . The line shape at the detector is roughly symmetric and approximately Gaussian, with a half-width at half maximum estimated to be around 0.01 \AA^{-1} . Owing to slit and beam stop imperfections the direct beam is not entirely blocked, which prevents reaching the nominal lower wave vector limit. The practical small wave vector limit of the recorded spectra is about 0.04 \AA^{-1} (for samples strongly scattering at small angles) or higher. The sample holders used are glass cylindrical capillaries from Glas (2 and 1.5 mm in diameter, 80 mm in length). They are sealed with a torch once filled with samples.

2.2.2. Light. — Dynamic light scattering is performed with a 72-channel, 4-bit digital correlator (Brookhaven Instruments) processing the signal of a photon-counting PMT (Hamamatsu). We use the red line (6471 \AA) of a Kr^+ laser source (Coherent), irradiating a sample immersed in a thermostated tank filled with CCl_4 as index matching liquid. The scattering angle may be varied from 20° to about 160° . When working with anisotropic (uniaxial) oriented samples, we may choose freely with our set-up the projection q_z of the scattering wave vector \mathbf{q} onto the optical axis direction. Our lamellar samples are oriented in glass capillaries (rectangular cross-section $2 \times 0.2 \text{ mm}^2$; length about 30 mm, from Vitrodynamics) through thermal treatment.

2.2.3. Neutrons. — The small-angle neutron scattering experiments were performed at the Laboratoire Léon-Brillouin in Saclay⁽¹⁾, with spectrometers PAXE and PAXY. The collimation is ensured by circular apertures (with beam diameter about 8 mm at the sample); the neutron wavelength λ is chosen by a mechanical selector ($\Delta\lambda/\lambda$ about 3%). On PAXE, the whole q -range is split into two configurations, with different sample-to-detector distances, yielding wave vector spans $7 \times 10^{-3} \text{ \AA}^{-1}$ to $6 \times 10^{-2} \text{ \AA}^{-1}$ and $7 \times 10^{-2} \text{ \AA}^{-1}$ to $5 \times 10^{-1} \text{ \AA}^{-1}$. The beam spots have widths, $\Delta q_0 = 1.5 \times 10^{-3} \text{ \AA}^{-1}$ and $2 \times 10^{-2} \text{ \AA}^{-1}$, respectively. On PAXY, the q -range extends from $6 \times 10^{-3} \text{ \AA}^{-1}$ to $4 \times 10^{-1} \text{ \AA}^{-1}$ with three configurations. The beam widths are $1 \times 10^{-3} \text{ \AA}^{-1}$, $2.8 \times 10^{-3} \text{ \AA}^{-1}$ and $5 \times 10^{-3} \text{ \AA}^{-1}$ as sample-to-detector distance is decreased. Samples are held in 1 or 2 mm quartz cells (Hellma).

3. Results

3.1. PHASE DIAGRAM. — The phase diagram of the ternary system water-octanol-SDS at constant temperature and pressure has been mapped out [11]. It exhibits a lamellar phase, which consists of a regular array of SDS-octanol membranes alternating with water layers. The extent of this phase can be described by the following two composition variables: membrane composition, defined as the molar octanol to SDS ratio R and membrane weight fraction c_m . The lamellar phase exists with R between 1.2 and 2.9, and c_m may be as low as 5%; the smectic period varies from a few nanometers up to 50 nm.

The representation of the phase diagram of the quaternary system water-PEG-SDS-octanol at fixed pressure and temperature requires one additional parameter. We use the polymer weight fraction in water c_p . In this paper, we restrict our study to a section of the phase diagram at fixed R , namely $R = 2.7$. Several hundred of samples were prepared to construct the phase diagram shown in Figure 1. In the composition range investigated, there is an isotropic liquid phase L , a lamellar phase L_α and three two-phase regions.

Salient features to emerge from this diagram are as follows. First, large amounts of polymer can be dissolved in the lamellar mesophase. For instance, a lamellar phase with a 40% membrane concentration may be swollen with a $c_p = 50\%$ polymer solution: *half* of the initial water can be replaced by polymer. Second, the polymer reduces the maximum swelling

⁽¹⁾ (Laboratoire commun CEA-CNRS)

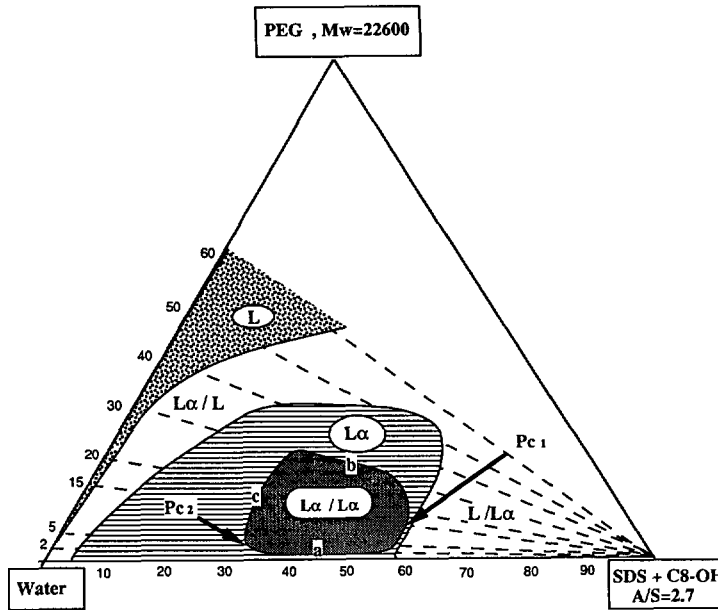


Fig. 1. — Section at constant temperature ($T = 25\text{ }^{\circ}\text{C}$) and membrane composition (octanol to SDS molar ratio $R = 2.7$) of the quaternary phase diagram water-octanol-SDS-PEG. Compositions are given as wt% fractions. The “membrane” corner corresponds to SDS and octanol. L is an isotropic phase, L_{α} a lamellar phase. L_{α}/L_{α} and other similar symbols represent two-phase domains. Pc_1 and Pc_2 are special points, discussed in the text below.

of the lamellar phase: when c_p is increased from 0 to 40%, the minimum c_m becomes five times higher. In contrast, the polymer has little effect on the membrane-rich side of the phase diagram: the boundary at high c_m is almost parallel to the polymer/water axis. At low c_m , part of the polymer is expelled as an aqueous solution (two-phase region L_{α}/L), whereas at high membrane fractions the separation arises between a lamellar phase and an octanol-rich solution, both phases containing polymer (L/L_{α} region). The presence of significant amounts of polymer in each of the coexisting phases is observed through NMR spectroscopy. Third, the most remarkable effect of the polymer is to produce at intermediate c_p and c_m values a closed-loop, two-phase region where two lamellar phases of different pitches coexist (L_{α}/L_{α}).

3.2. LAMELLAR PHASE. — A significant amount of information can be extracted from scattering experiments on lamellar phases. Structural and thermodynamic properties can be obtained from the positions and shapes of the Bragg peaks, respectively [10]. We have studied with X-ray scattering samples located along nine dilution lines, with c_p varying from 0 to 0.4. As an example, the X-ray scattering patterns for powder samples located along the dilution line $c_p = 0.005$ are displayed in Figure 2. The first and second harmonics of the structure factor are always observed (except for the most concentrated sample: its second harmonic is expected at 0.32 \AA^{-1} , i.e., outside the observed range); they move towards small angles as c_m decreases. At low c_m ($c_m < 0.30$) a third-order reflection becomes visible at the position expected for a lamellar phase.

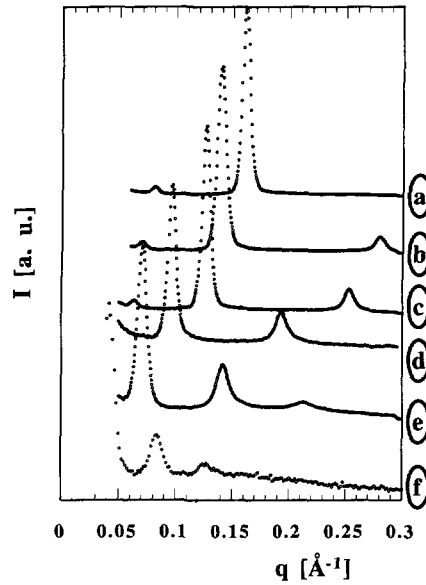


Fig. 2. — X-ray spectra at different membrane concentrations, along the dilution line defined by $c_p = 0.005$. Two or three diffraction peaks are seen, in the 1:2:3 ratio. Membrane weight fraction c_m is, from curve (a) to curve (f): 0.58, 0.50, 0.45, 0.35, 0.25, 0.15. The small-angle part of the signal for the most concentrated samples (a-c) is blurred by the presence of the λ/n harmonics from the monochromator.

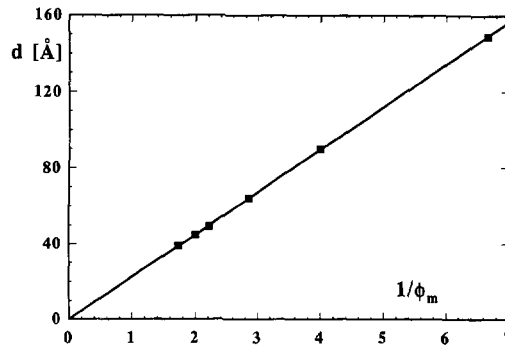


Fig. 3. — Smectic period $d \equiv 2\pi/q_0$ versus the inverse membrane volume fraction $1/\phi_m$, from X-ray spectra along the dilution line at $c_p = 0.005$. From the slope one gets the membrane thickness $\delta = 21.7 \text{ \AA}$.

Figure 3 is a plot of the smectic period d ($d = 2\pi/q_0$, with q_0 the position of the first order Bragg peak) as a function of $1/\phi_m$, with ϕ_m the membrane volume fraction⁽²⁾, for the dilution line at polymer content $c_p = 0.005$. The smectic period d follows the classical swelling law expected for a lamellar phase, namely $d = \delta/\phi_m$, which holds in the simple geometric model

⁽²⁾ The membrane volume fraction ϕ_m is deduced from the sample composition R , c_m and c_p , assuming that there is no polymer in the surfactant/alcohol bilayer. We use the following densities: $d_{\text{SDS}} = 1.16$, $d_{\text{octanol}} = 0.83$ and d_{solvent} ranging from 1 to 1.06 as c_p increases from 0 to 0.4.

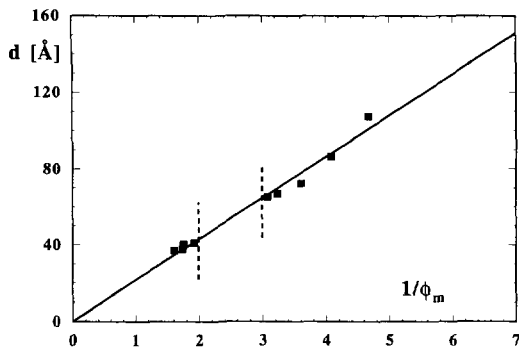


Fig. 4. — Smectic period d versus the inverse membrane volume fraction $1/\phi_m$, from X-ray spectra along the dilution line at $c_p = 0.30$. There is a gap for $0.3 \leq \phi_m \leq 0.5$, resulting from the L_α/L_α phase separation. The membrane thickness is $\delta = 20.9$ Å.

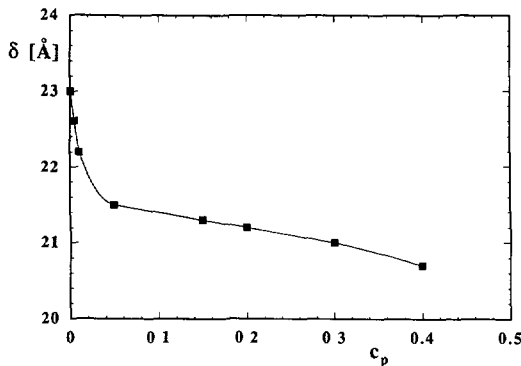


Fig. 5. — Evolution of the membrane thickness δ with the polymer weight fraction c_p .

of a periodic stack of flat objects with thickness δ and occupying a volume fraction ϕ_m . The geometric thickness is here $\delta = 22.6$ Å. The classical swelling law is also observed for all the other dilution lines, as long as the samples are located in the one-phase region of the phase diagram. When a dilution line crosses the two-phase region, as occurs for instance at $c_p = 0.3$, the slopes of the swelling laws for concentrated and dilute samples are the same, as illustrated in Figure 4.

The geometric thickness of the bilayer, as deduced from the swelling law depends on the polymer content. As shown in Figure 5, the thickness δ decreases from 23 Å in the polymer-free mesophase to 20.6 Å at $c_p = 0.4$. Most of the variation occurs at very low c_p ; further additions of polymer have little effect. With our assumption that polymer macromolecules are exclusively in water, the observed decrease of δ suggests a slight increase of the average area per polar head in the bilayer. A similar effect has been observed in the study of SDS micelles in the presence of PEG [2]. An alternative interpretation can be considered however: the observed decrease in the smectic period at constant surfactant-alcohol composition may also arise from a surfactant-like behaviour of part of the polymer, penetrating into the bilayer. At this stage, we cannot draw definite conclusions about the polymer distribution between solvent and bilayers

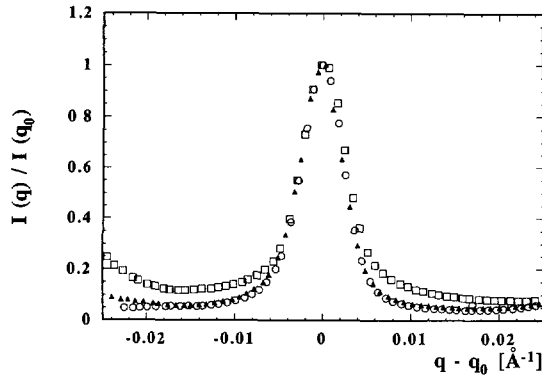


Fig. 6. — Neutron scattering data, normalized to peak intensity and centred to peak position q_0 , for three samples with the same membrane content $c_m = 0.10$ and different polymer concentrations. (○): $c_p = 0$; (▲): $c_p = 0.02$; (□): $c_p = 0.15$. Note that the addition of PEG leads to the appearance of tails at the bottom of the Bragg peak, indicating an increase in bilayer displacement fluctuations – increase in $\eta \propto 1/\sqrt{K\bar{B}}$ – and to the growth of the small angle scattering (proportional to $1/\bar{B}$).

As shown in Figure 6, the neutron scattering patterns are altered by the addition of polymer. For instance, along the line at $c_m = 0.10$ located far from the two-phase region of the phase diagram, it is observed that (i) broad tails appear at the bottom of Bragg peaks and (ii) small angle scattering appears as c_p increases. In the simpler case of two-component smectic liquid crystals, these two features of the scattering patterns are controlled by *elastic properties* of the system [10]: i) Bragg peaks exhibit power-law singularities and may therefore be broader than resolution. The power-law exponents are related to a dimensionless number η , defined in terms of the smectic elastic constants by [13]:

$$\eta = \frac{q_0^2 k_B T}{8\pi \sqrt{K\bar{B}}}$$

and ii) small angle scattering is inversely proportional to \bar{B} . In these expressions K is the smectic curvature modulus – related to the *bilayer* bending modulus κ and the smectic period d by $K = \kappa/d$ [14] – and \bar{B} the layer compressibility modulus – related to bilayer-bilayer interactions [10]. Then, if for our polymer-doped lamellar phase we assume similar dependences of the scattering patterns on the elastic constants, both features of our neutron scattering spectra may be qualitatively ascribed to a *decrease* of the elastic constant \bar{B} as the polymer content increases.

In order to further substantiate this last point, we attempted a quantitative determination of the layer compressibility modulus \bar{B} , using dynamic light scattering. In such an experiment, we measure the time behaviour of the auto-correlation function of the intensity of the light scattered by an oriented sample, as a function of both the magnitude and orientation of the scattering wave vector \mathbf{q} , for well-defined polarization states of the incident and scattered lights. Owing to serious problems in obtaining good-quality, oriented samples we have not been able to get results for more than one sample, with composition $\phi_m = 0.24$ and $c_p = 0.05$. The experiment was performed with the incident light polarized perpendicularly to the scattering plane, and without analyzing the polarization of the scattered light. With the sample holder used, the normal \mathbf{n} to the smectic layers was always contained within the scattering plane and the projection $q_z \equiv \mathbf{q} \cdot \mathbf{n}$ of the scattering wave vector was varied in the full accessible range, i.e. from zero to the modulus of \mathbf{q} . The dynamical part of the light scattering signal is quite

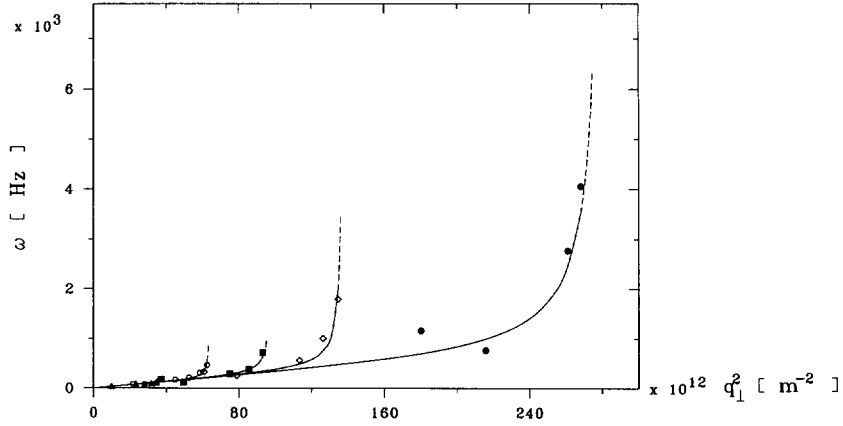


Fig. 7. — Relaxation frequency ω of the dynamic light scattering signal from an oriented one-phase sample, as a function of the projection q_{\perp} of the scattering wave vector \mathbf{q} . Five branches are displayed, corresponding to different values of the scattering angle φ : (\blacktriangle), $\varphi = 30^{\circ}$; (\circ), $\varphi = 40^{\circ}$; (\blacksquare), $\varphi = 50^{\circ}$; (\diamond), $\varphi = 60^{\circ}$; (\bullet), $\varphi = 90^{\circ}$. The sample composition is $c_p = 0.05 - \phi_m = 0.24$. The curves correspond to a single fit of the data to the anisotropic dispersion relation of the baroclinic mode, with fitted parameters: $\overline{B} = 1.9 \times 10^3$ Pa - $K \approx 1 \times 10^{-12}$ N. The curves are dashed in the q_{\perp} -range where there is no experimental data.

small. At large scattering angles, or for scattering wave vectors \mathbf{q} nearly parallel to the layers ($q_z \approx 0$) it disappears altogether. When detectable, the light scattering correlation function decays roughly as a single exponential. We thus analyzed its time relaxation in terms of a cumulant expansion, restricted to the first two terms.

In Figure 7 we plot the initial relaxation frequency ω as a function of q_{\perp}^2 , square of the component of the wave vector \mathbf{q} perpendicular to the optical axis \mathbf{n} ($q_{\perp}^2 = \mathbf{q}^2 - q_z^2$). The dispersion relation is clearly anisotropic: data taken at a given scattering angle - i.e. for a fixed *modulus* q of the scattering wave vector \mathbf{q} - denoted by a given symbol in Figure 7, depends on the *orientation* q_{\perp} of \mathbf{q} . We analyze this dispersion relation $\omega(q, q_{\perp})$ in terms of the undulation/baroclinic mode in two-component smectics [15, 16], neglecting in this first approach the polymer incidence on the dynamical properties of our system [17] and the weak polymer contribution to the light scattering signal. In this scheme, the light scattering signal arises from layer displacement fluctuations of membranes of constant thickness moving in a "background" solvent of non-fluctuating polymer composition. The relaxation frequency is then given by [10, 18]:

$$\omega = \frac{\overline{B}q_z^2 + Kq_{\perp}^4}{\eta_s q^4 + \frac{1}{\mu} q_z^2} q_{\perp}^2$$

where the elastic constants K and \overline{B} are the same as above, η_s is the solvent viscosity and μ the surfactant mobility, defined as: $\mu = d^2/12\eta_s$ [15].

Fitting the experimental data to this expression yields, taking η_s to be 3.8 mPa.s and the smectic period d - from X-ray scattering data - equal to 90 Å, a layer compression modulus $\overline{B} = 1.9 \times 10^3$ Pa and a curvature modulus K about 1×10^{-12} N. It should be noted that among these two values for the elastic constants only the value for \overline{B} is rather well-defined from the

experimental data, Figure 7: \bar{B} is associated to the limiting slope of the dispersion relation curves in the limit of small values for q_1^2 whereas K comes from the relaxation frequency at, or close to, $q_z = 0$ where experimental data is lacking.

The value we get experimentally for \bar{B} is strikingly smaller than the value that would be calculated in the case of the so-called *electrostatically-stabilized* lamellar phase – a system where charged bilayers have long-ranged, repulsive interactions through a solvent free from added salt. Indeed, in such systems one expects theoretically a layer compression modulus given by [19]:

$$\bar{B} = \frac{\pi}{2} \frac{k_B T d}{L_B (d - \delta)^3}$$

where L_B is the Bjerrum length of the solvent. With $L_B \approx 7 \text{ \AA}$ for water and the appropriate smectic period and bilayer thickness, 90 \AA and 21.5 \AA respectively, this formula yields: $\bar{B} \cong 3 \times 10^5 \text{ Pa}$. Our experimental value is also significantly smaller than the values measured in various electrostatically-stabilized lamellar phases with comparable smectic periods, where \bar{B} of the order of $1.5 \times 10^5 \text{ Pa}$ are found [20], always somewhat smaller than the theoretical value owing to weak screening by ionic impurities.

It may therefore be concluded from both phase diagram and scattering – neutron or light – data that the presence of the (non-ionic) polymer in our system leads to much less repulsive interactions between the surfactant bilayers than is usual with electrostatic systems. An attractive contribution to the interactions between the bilayers is indeed required in order to yield the observed phase separation between two lamellar systems [21].

3.3. L_α/L_α TWO-PHASE REGION. — As already mentioned, under particular conditions of polymer and membrane contents the quaternary mixtures water-SDS-octanol-PEG form two-phase equilibria involving two lamellar phases (Fig. 1). The identification of the two-phase region is quite difficult since there is no macroscopic phase separation, even using centrifugation presumably owing to the quite high viscosity of our samples. Moreover, polarizing microscopy is often unreliable because the two coexisting phases are both strongly birefringent and display the same lamellar textures. Therefore, the two-phase identification rests solely upon the analysis of the X-ray spectra: one-phase samples are characterized by their sets of Bragg peaks located at $q_0, 2q_0, 3q_0$, etc., with q_0 decreasing linearly as the membrane volume fraction ϕ_m decreases (Figs. 2-4), whereas two-phase samples display *two* distinct sets of Bragg peaks at $q_1, 2q_1, \dots$, and $q_2, 2q_2, \dots$. As an example, Figure 8 shows the evolution as c_m decreases of the X-ray spectra taken along the dilution line at $c_p = 0.20$. At high membrane concentrations, i.e. above $c_m = 0.55$, the X-ray spectra are those of one – phase lamellar samples; the same is true at membrane concentrations less than $c_m = 0.30$ (data in Figs. 8a, 8g). At intermediate membrane concentrations, the observed peaks are no longer simply related in reciprocal space (Figs. 8b-8f); however, they may be attributed to two coexisting lamellar phases with different smectic periods.

Using this procedure, two-phase samples are found in the central region of the lamellar domain: along dilution lines with polymer content in the range $0.01 \leq c_p \leq 0.35$, as well as varying the polymer concentration with membrane concentrations $0.30 \leq c_m \leq 0.55$. Since *one-phase* lamellar samples are always recovered for “extreme” compositions, with either c_p or c_m outside these bounds one may conclude that the two-phase domain is entirely included within the one-phase lamellar region of the phase diagram. Besides, the upper and lower boundaries of the two-phase domain (lines a and b in Fig. 1) follow very closely *dilution lines*, meaning that on these boundaries the polymer concentration in water is constant $c_p = 0.01$ and $c_p = 0.35$, respectively. Similarly, the left boundary (line c in Fig. 1) corresponds to a line at constant membrane fraction, $c_m = 0.30$. Note that along such a line the thickness of the

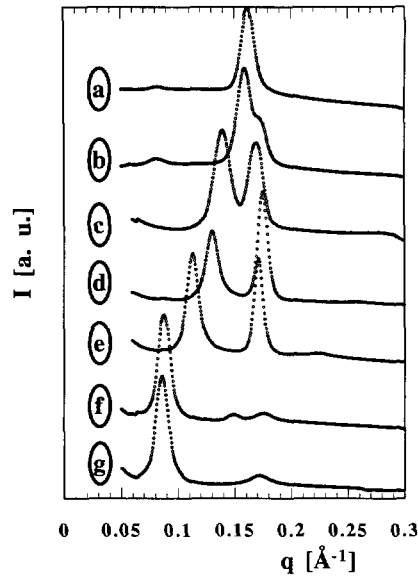


Fig. 8. — X-ray spectra for different membrane concentrations along the dilution line at $c_p = 0.20$. Membrane weight fraction c_m is, from curve (a) to curve (g): 0.55; 0.54; 0.50; 0.47; 0.42; 0.30; 0.28. For samples (b)-(f), two sets of Bragg peaks ratio are observed.

water layer ($d_w \approx 50 \text{ \AA}$, taking the membrane thickness to be $\delta \approx 20 \text{ \AA}$) is of the order of the diameter of isolated macromolecules ($2R_g = 58 \text{ \AA}$).

The closed-loop shape of the two-phase region would imply the presence of two critical points in a *three-component* system. Since we are dealing with a quaternary system, our case is *a priori* more complex: the membrane composition R may differ at both ends of a tie-line and, in particular, be different from the mean membrane composition $R = 2.7$. Unfortunately, a direct evaluation of the composition of the coexisting phases is impossible: we cannot achieve macroscopic phase separation. Therefore, the precise compositions of the coexisting phases – and in particular the polymer partitioning between the two lamellar phases – remain unknown.

However, some indications can be deduced from the splitting $\Delta q \equiv |q_2 - q_1|$ between the Bragg peak positions of the coexisting two lamellar phases. Large splittings are associated to strongly different lamellar phases while $\Delta q \rightarrow 0$ signals lamellar phases with negligible differences in smectic period, as should occur at a critical point. Mapping out the splitting Δq as a function of c_p and ϕ_m , we found two strong minima (i.e. a splitting smaller than the natural width of the lines) precisely located on the boundary of the two-phase domain, at $\phi_m = 0.58$, $c_p = 0.15$ and at $\phi_m = 0.32$, $c_p = 0.038$, respectively. It is tempting to think that these two points, denoted Pc1 and Pc2 in the phase diagram (Fig. 1) are, indeed, critical points – or close to critical points. Besides, upon approaching Pc2 at constant polymer content $c_p = 0.038$ from the one-phase side of the phase diagram it is observed on neutron spectra (see Fig. 9) a strong increase in small angle scattering signal and likewise in the Bragg peak width. This may be due to the vanishing of the layer compression modulus \bar{B} (equivalent to the diverging osmotic compressibility in isotropic solutions) as one gets closer to a smectic/smectic critical point [18, 22].

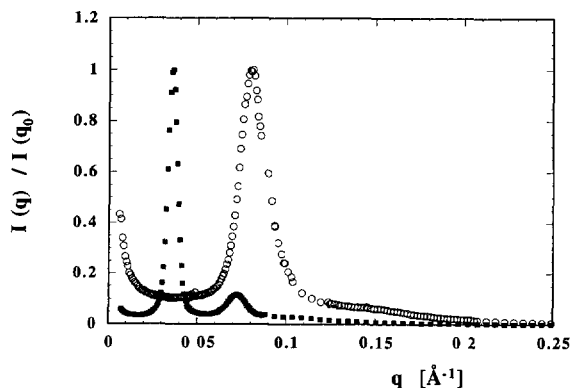


Fig. 9. — Evolution of the neutron scattering intensity (normalized to Bragg peak) in the vicinity of Pc2 and along the line at $c_p = 0.038$. The membrane concentration is 0.11 (■) or 0.26 (○). Broadening of the peaks and increase of the small angle scattering signal is observed, as would be the case if Pc2 were a critical point (the phase separation occurs at $c_m \approx 0.26$ with deuterated water).

4. Conclusion

In conclusion, our study shows that large amounts of a non-ionic polymer (polyethylene glycol) can be solubilized in an electrostatically-stabilized lamellar phase (sodium dodecylsulphate/octanol/water). Indeed, it is possible to replace up to 50% of the water contained in the lamellar phase with PEG. The maximum swelling of the lamellar phase is reduced by the presence of polymer. Moreover, for intermediate polymer concentrations and layer spacings adding polymer generates a closed-loop smectic-smectic miscibility gap that might be bounded by two critical compositions. The comparison with the polymer-free reference system shows that the presence of PEG slightly modifies the octanol-SDS bilayer. The moderate decrease of the repeat distance d induced by PEG may be due to either a thinning of the bilayer or a partial penetration of the polymer within it, or a combination of both effects. The interactions between bilayers are less repulsive in the presence of the polymer. They even become attractive enough to promote, for some polymer and membrane compositions, the phase separation between two smectic phases, with the possible existence of critical points.

Acknowledgments

We want to express our gratitude to Michael Cates and Didier Roux: they gave us encouragements in the course of theoretical discussions and by their enthusiastic attitudes. Warm thanks are also addressed to Roland Bernon, designer of our X-ray set-up: to his great proficiency and always kind assistance. We thank Monique Mauzac, Maryse Maugey and Oscar Babagbétó for their essential contribution to the characterization of the polymer. We also thank Patrick Kékicheff, for giving us helpful clues in the understanding of the queerness of some X-ray data. Finally, the help from the Laboratoire Léon-Brillouin (laboratoire commun CEA-CNRS) is gratefully acknowledged, especially from José Teixeira, Loïc Auvray and Annie Brûlet.

References

- [1] Robb I.D., Anionic Surfactants – Physico-Chemistry of Surfactant Action, *Surfactant Sci. Ser.* **11** E. Lucassen Reynders Ed. (Marcel Dekker, New York, 1981);
Goddard E.D., *Colloids Surf.* **19** (1986) 255;
Saito S., Nonionic Surfactants, M.J. Schick Ed. (Marcel Dekker, New York, 1987);
Hayakawa K. and Kwak J.C.T., Cationic Surfactants, D.N. Rubingh and P.M. Holland Eds. (Marcel Dekker, New York, 1991);
Goddard E.D., Interactions of Surfactants with Polymers and Proteins, E.D. Goddard and K.P. Ananthapadmanabhan Eds. (CRC Press, Boca Raton, 1993).
- [2] Cabane B. and Duplessix R., *J. Phys.* **43** (1982) 1529;
Cabane B. and Duplessix R., *J. Phys.* **48** (1987) 651.
- [3] Kékicheff P., Cabane B. and Rawiso M., *J. Coll. Int. Sci.* **102** (1984) 51.
- [4] De Gennes P.-G., *J. Phys. Chem.* **94** (1990) 8407.
- [5] Brooks J.T., Marques C.M. and Cates M.E., *J. Phys. II France* **1** (1991) 673.
- [6] Brooks J.T. and Cates M.E., *J. Chem. Phys.* **99** (1993) 5467.
- [7] Singh M., Ober R. and Kléman M., *J. Phys. Chem.* **97** (1993) 11108.
- [8] Ligoure C., Bouglet B. and Porte G., *Phys. Rev. Lett.* **71** (1993) 3600.
- [9] Bellocq A.-M. and Roux D., Microemulsions: Structure and Dynamics, S. Friberg and P. Bothorel Eds. (CRC Press, Boca Raton, 1986).
- [10] Roux D., Safinya C.R. and Nallet F., Micelles, Membranes, Microemulsions and Monolayers, W.M. Gelbart, A. Ben-Shaul and D. Roux Eds. (Springer-Verlag, New-York, 1994).
- [11] Auguste F., Ph.D. Thesis, Université Bordeaux-I (October 1993).
- [12] Ficheux M.-F., Nallet F. and Bellocq A.-M., unpublished results; the neutron scattering data were obtained at Laboratoire Léon-Brillouin, laboratoire commun CEA-CNRS.
- [13] Caillé A., *C. R. Acad. Sci. Paris* **B274** (1972) 891.
- [14] Helfrich W., *Z. Naturforsch.* **28c** (1973) 693.
- [15] Brochard F. and de Gennes P.-G., *Pramana Suppl.* **1** (1975) 1.
- [16] Nallet F., Roux D. and Prost J., *J. Phys. France* **50** (1989) 3147.
- [17] Nallet F., Roux D., Quilliet C., Fabre P. and Milner S.T., *J. Phys. II France* **4** (1994) 1477.
- [18] Sigaud G., Garland C.W., Nguyen H.T., Roux D. and Milner S.T., *J. Phys. II France* **3** (1993) 1343.
- [19] Roux D. and Safinya C.R., *J. Phys. France* **49** (1988) 307.
- [20] Parsegian V.A., Rand R.P. and Fuller N.L., *J. Phys. Chem.* **95** (1991) 4777;
Dubois M., Zemb Th., Belloni L., Delville A., Levitz P. and Setton R., *J. Chem. Phys.* **96** (1992) 2278.
- [21] Wennerström H., Physics of Amphiphilic Layers, J. Meunier, D. Langevin and N. Boccara Eds. (Springer-Verlag, Berlin, 1987).
- [22] Zemb Th., Gazeau D., Dubois M. and Gulik-Krzywicki T., *Europhys. Lett.* **21** (1993) 759.